Coordination Chemistry of *N*,*N*,*N*′,*N*′-Tetraethylpyridine-2,6-dithiocarboxamide (*S*-dept) – X-ray Crystal Structures and Magnetic Properties of [Co(*S*-dept)X_2] (X = Br, I, and NCS)

Ramesh Kapoor,*[a] Ashok Kataria,[a] Paloth Venugopalan,[a] Pratibha Kapoor,[a] Geeta Hundal,[b] and Montserrat Corbella*[c]

Keywords: *N*,*N*,*N*′,*N*′-Tetraethylpyridine-2,6-dithiocarboxamide / X-ray crystallography / IR / Zero-field splitting / EPR

Mononuclear cobalt(II) complexes [Co(*S*-dept)X_2] [X = Br (**1**), I (**2**) and NCS (**3**)] were synthesized using *N*,*N*,*N*′,*N*′-tetraethylpyridine-2,6-dithiocarboxamide (*S*-dept), and characterised by conductivity, spectral and single-crystal X-ray diffraction studies. These studies reveal that the compounds consist of discrete monomeric molecules in which the cobalt atoms are five-coordinate in an environment that is best described as being distorted square-pyramidal. In dimethylformamide the iodo complex shows significant ionic dissociation (1:1 electrolyte) and its crystal field absorption spectrum is interpretable in terms of an octahedral structure [Co(*S*-dept)$(DMF)_2$I]$^+$. The temperature dependence of the magnetic susceptibility data is indicative of a high-spin compound with an important zero-field splitting. The best fit was obtained with $|D| = 20.5\ cm^{-1}$ and $g = 2.53$ for **1**, $|D| = 14.2\ cm^{-1}$ and $g = 2.38$ for **2** and $|D| = 17.7\ cm^{-1}$ and $g = 2.35$ for **3**. The X-band EPR spectra at low temperature is also characteristic of an $S = 3/2$ state with important zero-field splitting. The most important band appears at low fields (ca. 1200 G).

Introduction

There has been a growing interest in the development of coordination chemistry of nonmacrocyclic multidentate ligands derived from pyridine-2,6-dicarboxylic acid (I).[1,2] The symmetrical tertiary amide side arms at the 2- and 6-positions of the central pyridine ring provide a variety of novel *ONO*-tridentate receptors for binding to metal ions (II).[2] The inflexibility of the ligand in these systems has been one of the important factors leading to the isolation of low-symmetry five-coordinate complexes of Cu^{II}, Co^{II}, Ni^{II}[3–6] and nine-coordinate complexes of lanthanide ions.[2] Steric and electronic consequences brought by peripheral substitutions to the terminal carboxamide side arms have been well illustrated by Piguet et al.[2] on the complexation of Ln^{III} ions. Recently, we have extended these studies to ligands containing C=S instead of C=O bonds on the side arms at the 2- and 6-positions, i.e., ligands containing an *SNS* set of donor atoms (III).[7,8] Deviations from idealized geometries would be naturally expected because of the bulky alkyl groups on the nitrogen atoms and may cause structural constraints. *N*,*N*,*N*′,*N*′-Tetraethylpyridine-2,6-dithiocarboxamide [R^1, R^2 = Et in (III); *S*-dept] coordinates through the planar *SNS* set of donor atoms. Our recent studies on (*S*-dept)$_2MCl_2$ (M = Co and Cu) complexes have revealed significant structural differences between the two complexes.[7,8] The copper complex is composed of cationic and anionic dimers: $[Cu_2Cl_2(\mu$-*S*-dept$)_2][Cu_2Cl_4(\mu$-Cl$)_2]$. The cationic fragment exhibits an unusual Cu–Cu disposition taking place through bridging sulfur atoms, observed only in a few Cu^{II} complexes.[8] The coordination geometry around each Cu center is approximately distorted square-pyramidal. On the other hand, the cobalt complex[7] is built up of [Co(*S*-dept)(Cl)]$^+$ and $[Co_2Cl_4(\mu\text{-}Cl)_2]^{2-}$ ions. The cobalt ion in the cation has a distorted square-planar geometry. The cationic units are stacked over each other in a staggered manner so that each cobalt ion interacts weakly with a sulfur atom of a unit above and below it.

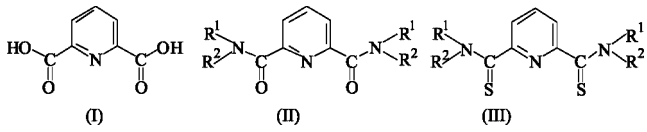

Spectrophotometric, magnetic and electrical conductivity measurements had been reported for a large number of five-coordinate complexes of cobalt(II).[9–27] In most cases, the magnetic moment was only measured at room temperature, in order to determine the spin-sate of the system [high-spin ($S = 3/2$) or low-spin ($S = 1/2$)]. For some compounds the

[a] Department of Chemistry, Panjab University, Chandigarh 160014, India
[b] Department of Chemistry, Guru Nanak Dev University, Amritsar 143005, India
[c] Departament de Química Inorgànica, Facultat de Química, Universitat de Barcelona, 08028 Barcelona, Spain

  DOI: 10.1002/ejic.200500318

magnetic measurements at different temperatures were reported but not the X-ray crystal structure.[20,21] In other cases, the X-ray crystal structure was reported, but not the study of $\chi_M = f(T)$.[9–13,24,25,27,28]

To the best of our knowledge, very few high-spin five-coordinate Co^{II} complexes are structurally and magnetically characterized. Some of them are polynuclear systems[29–32] and their magnetic properties are due to the interaction between the Co^{II} ions. Only 3 mononuclear complexes are reported in the literature with the structural data and magnetic study (χ vs. T): [Co{(*t*Bu)(Me)salmdptn}],[22] [Co(saloph)(2-MeImd)][23] and $[Co(L^5)_2(H_2O)]$[26] with HL^5 = *N*-(2-chloro-6-methylphenyl)pyridine-2-carboxamide.

In this paper, we describe the crystal structure and magnetic properties of [Co(*S*-dept)X_2] (X = Br, I and NCS) compounds. The present work is aimed to determine the steric influence of the *SNS* set of donor atoms of *S*-dept on the geometry of the complexes. Our studies have revealed significant structural differences between [Co(*S*-dept)-$(NCS)_2$] and its nickel analogue.[33]

Five-coordinated mononuclear Co^{II} (d^7) complexes can be high-spin (S = 3/2), low-spin (S = 1/2) or a temperature-induced spin-transition can be observed. For high-spin Co^{II} complexes the study of the magnetic properties allows to find the value of the zero-field splitting parameters. In this work, we report the temperature dependence of the magnetic susceptibility and the fit of the experimental data allows finding the parameters of the zero-field splitting. The EPR spectra in frozen solution is also reported.

Results and Discussion

These complexes are obtained in good yield by mixing equimolar amounts of *S*-dept and the appropriate salt in anhydrous EtOH. The compounds are air- and moisture-stable and are readily soluble in the common organic solvents such as $CHCl_3$, CH_2Cl_2, and 1,2-dichloroethane. The tridentate nature of the ligand and the fact that the complexes are practically undissociated in chloroform and dichloromethane solutions suggest penta-coordination around the metal ion in these solvents. In CH_3CN and DMF solutions, the iodo complex **2** shows significant dissociation and molar conductivities are in the range typical of 1:1 electrolytes.[35] The complex most probably ionizes to give $[Co(S\text{-dept})I]^+_{solv}$ and I^- in these solutions. The conductivity data clearly show that the dissociation is less extensive for the bromo and thiocyanato complexes and molar conductivities are significantly less than the values expected for 1:1 electrolytes.

The expected positive shifts in position and changes in intensity of the principal IR bands of the pyridine ring are interpreted in favour of the coordination of *S*-dept through the pyridine ring nitrogen atom[36] in the complexes. Bands at 1263, 990, and 818 cm^{-1} may be considered as having significant contribution from C=S vibrations, based on comparison of the spectra of *O*-deap and *S*-dept. These bands show a slight downward shift in frequency in these complexes indicating coordination of the sulfur atoms. The presence of a band at 2062 cm^{-1} in **3** is consistent with *N*-bonded terminal thiocyanato groups.[37] The corresponding ν(CS) modes are obscured by ligand vibrations.[38,39]

The close similarity between the crystal-field spectra of the solid compounds (Br and NCS derivatives) and of their solutions in $CHCl_3$ indicates that these compounds retain the same structure (see Table 4). Compounds **1**, **2**, and **3** each show four distinct bands which are consistent with five-coordinate high-spin cobalt(II) complexes.[14–16] The spectra can be correlated with those of the complexes Co(MABenNEt_2)Cl_2,[17] Co(Et_4dien)X_2 (X = Cl, Br, I, N_3, and NCS),[15] Co(Me_5dien)Cl_2[18,19] and Co(Et_4dien)Cl_2.[11] The complexes **1**–**3** show a common band at ca. 625 nm which is assigned to the $^4A_{2'}(F) \rightarrow {}^4A_{2'}(P)$ transition. This band is characteristic of five-coordinate complexes irrespective of the nature of the donor atoms and the true geometry of the complex.[16] Their electronic spectra also show solvent dependence. In DMF solutions, the spectra are consistent with Co^{II} in an octahedral configuration, probably formed by coordination of DMF. In DMF solution, the iodo complex is, however, strongly conducting, probably one of the iodine atoms is dissociated to give [Co(*S*-dept)$(DMF)_2I]^+$ and free iodide ions. Complexes **1** and **3** are non-conducting in DMF and may be formulated as [Co(*S*-dept)(DMF)X_2] (X = Br and NCS).

Crystal Structures of [Co(S-dept)X_2] [X = Br (1), I (2), and NCS (3)]

The molecular structures and the atom labelling scheme of the complexes are shown in Figures 1, 2, and 3. Selected bond lengths and angles are listed in Table 1. The three complexes consist of monomeric molecules with a five-coordinate stereochemistry resulting from bonding to terdentate *S*-dept ligand and the other two positions are occupied by two X groups (Br, I or terminal *N*-bonded NCS). The geometry about the cobalt atom may be described either as square-pyramidal or trigonal-bipyramidal, depending on the parameter, $\tau = \beta - \alpha/60$ (β is defined as the larger of the basal angles and α is the remaining angle).[39] When τ is 0, the coordination is square-pyramidal; however for a trigonal-bipyramidal configuration τ is 1, and is often reported as a percent value. The τ values for **1** [β = N(1)–Co(1)–Br(2), 159.66(17)° and α = S(2)–Co(1)–S(1), 137.96(9)°], **2** [β = N(1)–Co(1)–I(2), 166.19(12)° and α = S(1)–Co(1)–S(2), 131.58(7)°], and **3** [β = N(5)–Co(1)–N(1), 164.27(18)° and α = S(1)–Co(1)–S(2), 138.76(6)°] are 36.2, 57.7, and 42.5%, respectively. Complexes **1**–**3** may be considered as distorted square-pyramidal. The anions differ in the angles with the metal atom which destroys the two-fold rotational symmetry of the molecules. The torsion angles between the pyridine ring (C1,C2,C3,C4,C5 and N1) and the thioamide planes (C1,C6,S1,N2 and C5,C11,S2,N3) are: 45.4(1) and 35.9(1) for **1**, 38.8(1) and 35.9(1) for **2**, and 38.8(1) and 52.1(1) for **3**. There appears to be no correlation between the angle of rotation of thioamide groups and the pyridine

ring. However, the conformation of the ligand seems to be dependent on the size of the anion. The conformation of iodide and thiocyanate complexes are almost identical with methyl carbon atoms C13 and C15 being on the same side of the amide group, whereas C8 and C10 are on opposite sides of the plane. In the case of the bromide complex the methyl groups C8 and C10 as well as C13 and C15 are on the opposite sides with respect to the thioamide plane.

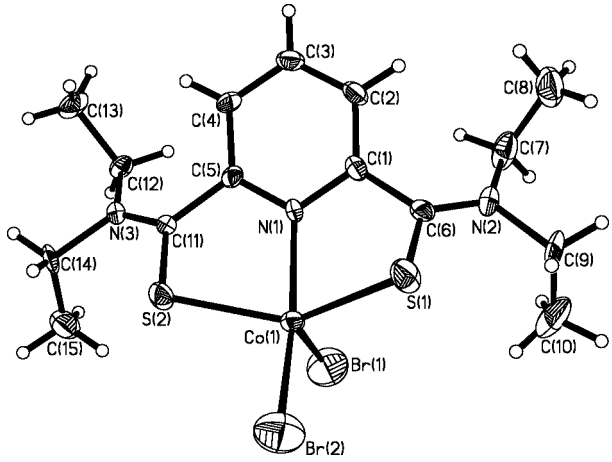

Figure 1. Perspective view of complex **1** with atom numbering scheme (thermal ellipsoids at 50% probability level).

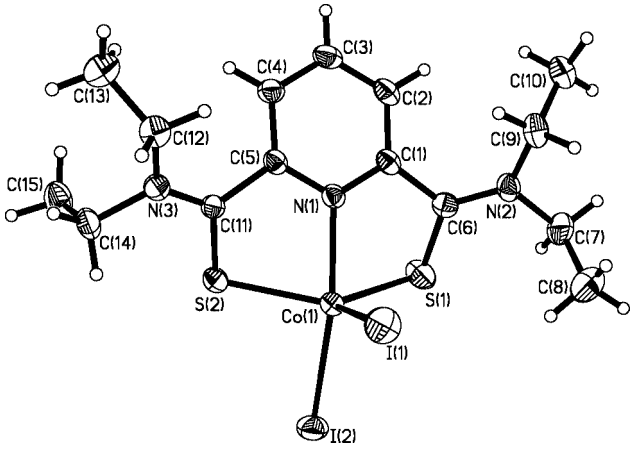

Figure 2. Perspective view of complex **2** with atom numbering scheme (thermal ellipsoids at 50% probability level).

In the structure of **1** the bromine atom Br(1) occupies the apical position and sulfur atoms S(1), S(2), pyridine N(1) and Br(2) form the base of the pyramid. The mean plane through these atoms indicates that the atoms are 0.205, 0.203, –0.238, and –0.170 Å, respectively, above and below the mean plane. The Co ion is –0.607 Å below the mean plane defined by these four atoms. Similarly, in the structure of **2** the iodine atom I(1) occupies the apical position and sulfur atoms S(1), S(2), pyridine N(1) and I(2) form the base of the pyramid. The mean plane through these atoms indicates that the atoms are 0.307, 0.328, –0.396, and –0.239 Å, respectively, above and below the mean plane. The Co ion is –0.599 Å below the mean plane defined by these four atoms.

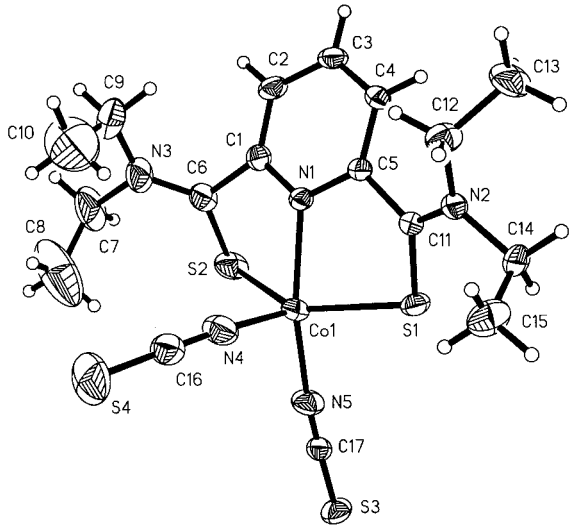

Figure 3. Perspective view of complex **3** with atom numbering scheme (thermal ellipsoids at 50% probability level).

Table 1. Selected bond lengths [Å] and angles [°] for complexes **1**–**3**.

Complex **1**			
Br(1)–Co(1)	2.3985(15)	Br(2)–Co(1)	2.4121(15)
Co(1)–N(1)	2.150(6)	Co(1)–S(2)	2.365(2)
Co(1)–S(1)	2.368(2)	S(1)–C(6)	1.708(8)
S(2)–C(11)	1.696(7)		
N(1)–Co(1)–S(2)	80.14(15)	N(1)–Co(1)–S(1)	81.06(15)
S(2)–Co(1)–S(1)	137.96(9)	N(1)–Co(1)–Br(1)	91.73(16)
S(2)–Co(1)–Br(1)	109.03(7)	S(1)–Co(1)–Br(1)	108.79(8)
N(1)–Co(1)–Br(2)	159.66(17)	S(2)–Co(1)–Br(2)	93.91(6)
S(1)–Co(1)–Br(1)	90.94(7)	Br(1)–Co(1)–Br(2)	108.58(5)
C(6)–S(1)–Co(1)	94.9(2)		
Complex **2**			
I(1)–Co(1)	2.6156(9)	I(2)–Co(1)	2.7065(9)
Co(1)–N(1)	2.137(5)	Co(1)–S(1)	2.3574(18)
Co(1)–S(2)	2.3799(17)	S(1)–C(6)	1.714(6)
S(2)–C(11)	1.709(6)		
N(1)–Co(1)–S(1)	80.17(13)	N(1)–Co(1)–S(2)	79.99(12)
S(1)–Co(1)–S(2)	131.58(7)	N(1)–Co(1)–I(1)	89.55(12)
S(1)–Co(1)–I(1)	107.42(6)	S(2)–Co(1)–I(1)	116.11(5)
N(1)–Co(1)–I(2)	166.19(12)	S(1)–Co(1)–I(2)	98.69(5)
S(2)–Co(1)–I(2)	90.87(4)	I(1)–Co(1)–I(2)	103.83(3)
C(6)–S(1)–Co(1)	95.61(19)	C(11)–S(2)–Co(1)	96.37(19)
Complex **3**			
Co(1)–S(2)	2.3979(16)	Co(1)–S(1)	2.3777(15)
N(4)–Co(1)	1.964(5)	N(5)–Co(1)	2.003(5)
N(1)–Co(1)	2.134(4)	C(17)–S(3)	1.612(5)
C(17)–N(5)	1.147(6)	C(16)–S(4)	1.609(7)
C(16)–N(4)	1.149(7)	C(6)–S(2)	1.682(6)
C(11)–S(1)	1.698(4)		
N(4)–Co(1)–N(5)	102.1(2)	N(4)–Co(1)–N(1)	93.57(18)
N(5)–Co(1)–N(1)	164.27(18)	N(4)–Co(1)–S(1)	114.34(17)
N(5)–Co(1)–S(1)	94.34(14)	N(1)–Co(1)–S(1)	80.03(10)
N(4)–Co(1)–S(2)	103.34(17)	N(5)–Co(1)–S(2)	93.56(15)
N(1)–Co(1)–S(2)	81.56(10)	S(1)–Co(1)–S(2)	138.76(6)
C(11)–S(1)–Co(1)	98.48(16)	C(6)–S(2)–Co(1)	91.50(18)

The isothiocyanate nitrogen atom N(4) occupies the apical position and sulfur atoms S(1) and S(2), pyridine N(1) and thiocyanate N(5) form the base of the pyramid. The mean plane through N(1), N(5), S(1), S(2) indicates that these atoms are 0.39, 0.52, –0.05, –0.08 Å, respectively, above and below the mean plane. The Co ion is 0.74 Å above the mean plane defined by these four atoms. It is interesting that the Co–NCS linkages in **3** are bent with Co–N(5)–C(17) and Co–N(4)–C(16) angles of 171.0(5) and 167.0(6), respectively. It has been observed by others[40,41] that this linkage may be either linear or angular, with examples of M–N–C angles falling in the range 141–174°. The non-linearity of this type may be attributed to steric factors.[21] It also suggests electron density localisation on the donor nitrogen atom such that a canonical form **I** contributes to the structure.[40,42]

Co

I

It has been known that interactions of cobalt and nickel thiocyanates with terdentate ligands provide complexes of different stereochemistry.[35,43] Our present results provide ample evidence that cobalt has a greater tendency than nickel to give monomeric five-coordinate complexes rather than octahedral complexes.

Extended Hückel Calculations

The compounds reported here show a $CoNS_2X_2$ core, with significant differences in the Co–ligand distances. Compound **3** shows a CoN_3S_2 core, with three short Co–N distances (ca. 2.1 Å) and two long Co–S (ca. 2.4 Å) (*x*-axis) distances (see Scheme 1). Compound **1**, with a $CoNBr_2S_2$ core, has one short Co–N (ca. 2.1) and four long Co–S and Co–Br (ca. 2.4 Å) (*yz*-plane) distances. Finally, for compound **2** with a $CoNI_2S_2$ core, we observe one short Co–N (ca. 2.1 Å), two long Co–S (ca. 2.4 Å) (*x*-axis), and two very long Co–I distances with values in the range ca. 2.6–2.7 Å. Then, from the point of view of bond lengths, compound **3** shows a more regular core, with short Co–L distances, while compound **2** shows the most irregular core, with long Co–L distances.

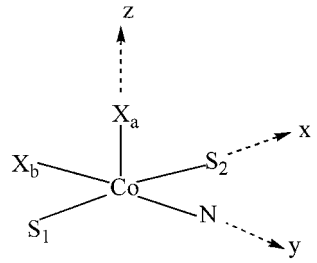

Scheme 1.

Extended Hückel calculations with the crystallographic coordinates of compounds **1**–**3** were carried out with the CACAO program.[44] Due to the absence of symmetry in these complexes a full split of the five d orbitals is obtained and a great delocalisation towards the ligands is observed in all cases. There are at least nine MOs with a cobalt contribution >15%.

High-spin Co^{II} compounds show three singly occupied molecular orbitals (SOMOs). The highest energy SOMO shows a significant contribution of the $x^2 - y^2$ orbital of the cobalt ion and has a σ*-character with the ligands in the basal plane (S_1, N, S_2, and X_b), while the next SOMO is constituted essentially by the z^2 of the cobalt ion and the p orbital of the monodentate ligand in apical position (X_a) (or the non-bonding π_{nb} orbital of the NCS ligand). The lowest energy SOMO shows a significant contribution of the *xz* orbital of the Co^{II} ion and of the p orbitals of S_1 and S_2. In the iodide complex (and in minor proportion in

Table 2. Energy and composition[a] of the three SOMOs for compounds **1**–**3**.

	Energy	% Co	% N	% S1	% S2	Xb	Xa
Compound **1**							
σb*	–10.258	33 (x^2–y^2); 3 (z^2); 3 (*yz*)	15	6	6	14	–
σa*	–11.572	41 (z^2); 6 (*pz*)	2	–	4	–	22
π*	–11.775	28 (*xz*); 8 (*xy*); 4 (*px*)	–	17	19	2	6
Compound **2**							
σb*	–10.430	32 (x^2–y^2); 5 (z^2)	18	4	5	17	2
σa*	–11.646	32 (z^2); 5 (x^2–y^2); 5 (*pz*)	–	8	4	2	26
π*	–11.783	27 (*xz*); 7 (*xy*); 4 (*px*)	–	17	16	3	11
Compound **3**							
σb*	–10.243	38 (x^2–y^2); 7 (z^2)	17	6	5	6	–
σa*	–11.690	46 (z^2); 5 (x^2–y^2); 6 (*pz*)	–	6	7	–	8
π*	–11.878	24 (*xz*); 6 (*xy*); 2 (z^2); 3 (*px*)	–	17	23	–	–

[a] See Scheme 1.

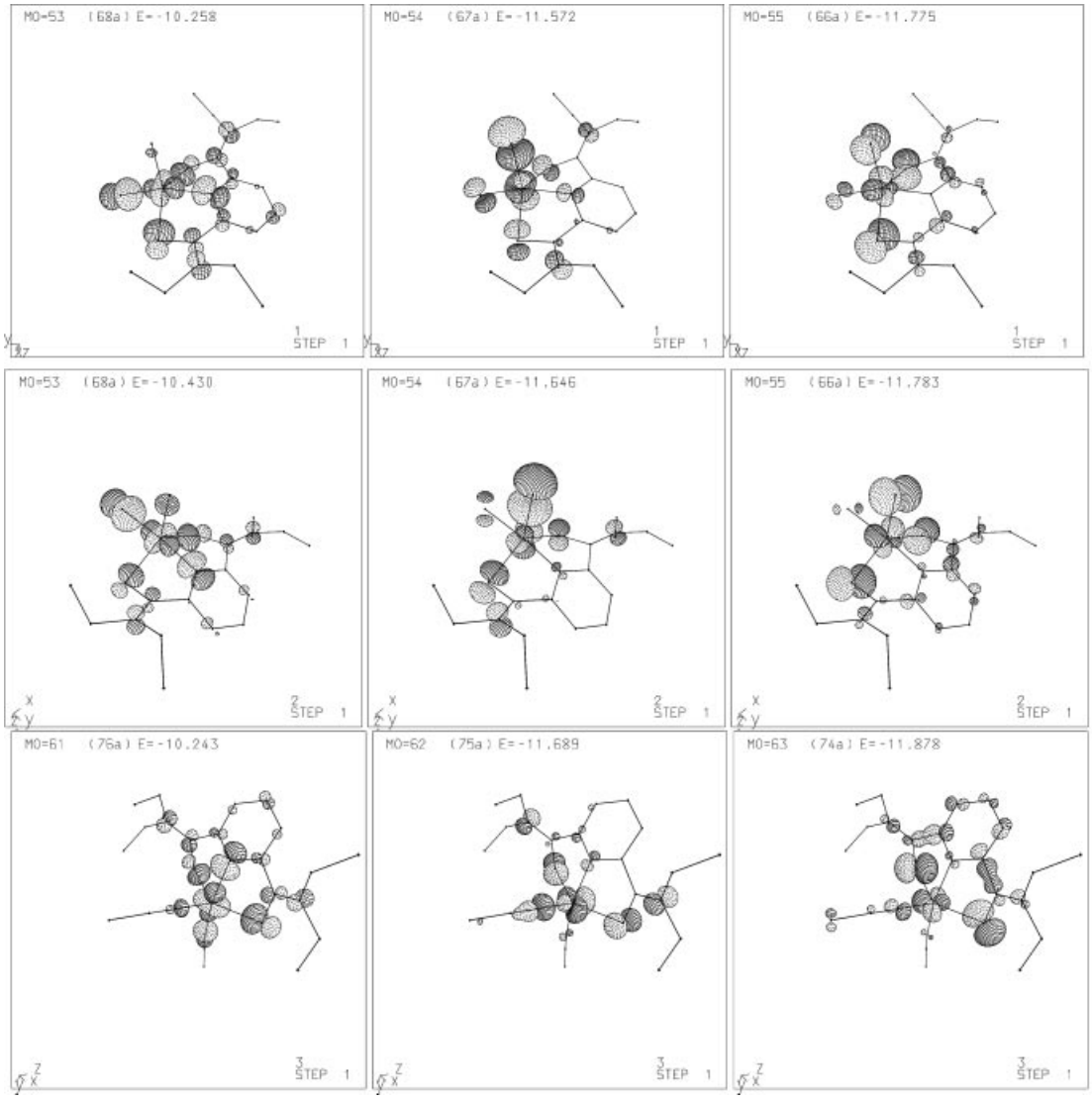

Figure 4. SOMOs for compound **1** (top), **2** (centre), and **3** (bottom).

the bromide complex) a considerable contribution of the apical ligand is also observed (Table 2, Figure 4).

Due to the distortions in the geometry, the *xz*, *yz*, and *xy* orbitals of the Co^{II} ions contribute to several MOs. However, these results confirm the description of the structure of these compounds as a distorted square pyramid. The energy of σ_a* is similar for the three compounds, while σ_b* is more stabilized for compound **2**, which shows a major distortion to the trigonal-bipyramidal geometry, than for **1** and **3** (Figure 5).

One of the limitations of the extended Hückel calculations is the non-inclusion of the inter-electronic repulsions; nevertheless, from a qualitative point of view, we can consider for each compound, a similar pairing energy in each orbital, and from the energy diagram shown in Figure 5, we can find an approximate value for the relative energies of the different excited states (E1–E6). From these results, we can propose, for the three compounds, the presence of several excited states close in energy to the ground state (ca. 5000 cm^{-1}, E1–E3 and E4) (Table 3). These states would

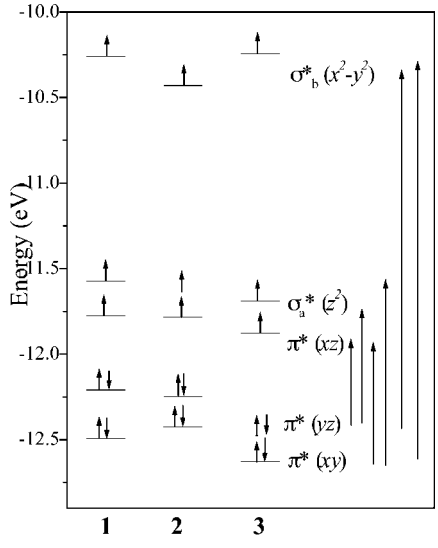

Figure 5. MO energy diagram for compounds **1**–**3**.

correspond to the different transitions $\pi^* \rightarrow \pi^*$ and $\pi^* \rightarrow \sigma a^*$ (z^2), and the transition $\pi^* \rightarrow \sigma b^*$ ($x^2 - y^2$) should appear at higher energy (ca. 16000 cm^{-1}).

Table 3. Relative Energy [10^{-3} cm^{-1}] of the different excited states proposed for compounds **1**–**3**.

		1	**2**	**3**
$(xy)(yz)^2(xz)(z^2)(x^2–y^2)^2$	E6	17.6	15.8	19.0
$(xy)^2(yz)(xz)(z^2)(x^2–y^2)^2$	E5	15.6	14.6	16.8
$(xy)(yz)^2(xz)(z^2)^2(x^2–y^2)$	E4	7.1	6.1	7.4
$(xy)(yz)^2(xz)^2(z^2)(x^2-y^2)$	E3	5.5	5.0	5.9
$(xy)^2(yz)(xz)(z^2)^2(x^2–y^2)$	E2	5.1	4.8	5.2
$(xy)^2(yz)(xz)^2(z^2)(x^2–y^2)$	E1	3.5	3.7	3.7
$(xy)^2(yz)^2(xz)(z^2)(x^2–y^2)$	E0	0	0	0

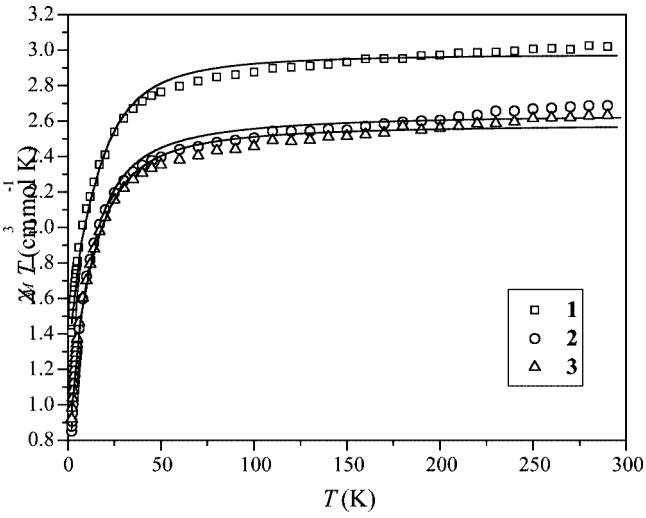

Figure 6. $\chi_M T$ vs. T plot for **1**–**3**. The solid line is the best fit to the experimental data.

Magnetic Properties

The magnetic susceptibility of **1**–**3** was measured in the range 2–300 K (Figure 6). In all cases, the $\chi_M T$ product decreases with the temperature. The shape of the three graphs is similar, but for compound **1**, we found higher $\chi_M T$ values. The room-temperature values of $\chi_M T$ = 3.03 cm^3 mol^{-1} K (for **1**) and 2.7 cm^3 mol^{-1} K (for **2** and **3**) differ from the spin-only value $\chi_M T$ = 1.87 cm^3 mol^{-1} K for S = 3/2 (high-spin Co^{II} complexes) which indicates an orbital contribution to the g-values. On lowering the temperature, $\chi_M T$ decreases, and under 50 K $\chi_M T$ falls drastically. The shape of the $\chi_M T$ vs. T graph is indicative of an important zero-field splitting. Owing to spin-orbit coupling, the S = 3/2 state is split into two Kramer's doublets ($M_s = \pm 1/2, \pm 3/2$), separated by 2D, with D being the axial zero-field splitting parameter. Formally, the magnetic behaviour can be treated as an S = 3/2 spin state under the action of the spin Hamiltonian $H = D[S_z^2 - S(S + 1)/3] + g_{\parallel}\beta Hz S_z + g_{\perp}\beta(H_x S_x + H_y S_y)$. The expression of the magnetic susceptibilities χ_M [with $\chi_M = (\chi_{\parallel} + 2\chi_{\perp})/3$] is derived from this Hamiltonian.[45] With the aim to fit the low-temperature values, it was necessary to modify the equation, including the term of the intermolecular magnetic interactions zJ, where J is the interaction parameter between two nearest neighbour magnetic species and z is the number of nearest neighbours around a given magnetic molecule in the crystal lattice. Then the equation used to fit the experimental data is

$$\chi_M T = \frac{TNg^2\beta^2 F(D,T)}{3kT - zJ \cdot F(D,T)}$$

where

$$F(D,T) = \frac{1}{4}\left[\frac{1+9\exp(-2D/kT)}{1+\exp(-2D/kT)}\right] + 2kT\left(\frac{(\frac{1}{kT}) + \frac{3}{4D} - \frac{3}{4D}\exp(-2D/kT)}{1+\exp(-2D/kT)}\right)$$

The best fits were obtained with $|D|$ = 20.5 cm^{-1}, g = 2.53, zJ = –0.50 cm^{-1} and $R = 1.8 \cdot 10^{-4}$ (**1**); $|D|$ = 14.2 cm^{-1}, g = 2.38, zJ = –1.67 cm^{-1} and R = 2.7 10^{-4} (**2**); $|D|$ = 17.7 cm^{-1}, g = 2.35, zJ = –1.23 cm^{-1} and R = 2.9 10^{-4} (**3**). As it can be seen in Figure 6, compounds **2** and **3** show similar $\chi_M T$ values, while compound **1** shows at room temperature a higher $\chi_M T$ value, indicative of a large g value. The best fit of the experimental data also corresponds to a largeer D value for **1** than for **2** or **3**.

As it has been indicated, very few high-spin five-coordinate Co^{II} complexes are structurally and magnetically characterized. Only three mononuclear complexes are reported in the literature with the structural data and magnetic study (χ vs. T): [Co{(*t*Bu)(Me)salmdptn}] (with D = –38.9 cm^{-1}, E = 1.7 cm^{-1}, g_x = 1.68, g_y = 1.89, g_z = 3.21 and zJ = –1.0 cm^{-1}),[22] [Co(saloph)(2-MeImd)] (with $|D|$ = 22.6 cm^{-1}, g = 2.14),[23] and [Co(L^5)$_2$(H_2O)] with HL^5 = *N*-(2-chloro-6-methylphenyl)pyridine-2-carboxamide (Curie–Weiss law between 80–300 K).[26] The study of the magnetic properties of [Co(Salpad)$_2$(t-MeStpy)] (D = 16.57 cm^{-1}, g = 2.39),[20] [Co(H_2fsa)$_2$(phn)(t-MeStpy)] (spin equilibrium),[20] and [Co(bzimpy)Cl_2] (D = 73.4 cm^{-1}, E = 3.28 cm^{-1}, zJ = –0.205 cm^{-1})[21] are also reported in the literature, but to the best of our knowledge, the crystal structure of these compounds is not published.

In spite of the limited number of mononuclear Co^{II} compounds with five-coordination which have been structurally and magnetically characterized, two facts could be discussed: the stabilization of the spin state S = 3/2 and the magnitude of the zero-field splitting.

Cobalt(II) complexes with Schiff-base ligands could be high-spin or low-spin. In a comparative study of five-coordinate Co^{II} complexes of the types [Co(salen)L] and [Co(saloph)L] reported by Kennedy et al.,[23] the authors note an increase of the out-of-plane displacement of the Co^{II} ion from ca. 0 Å for low-spin complexes to ca. 0.45 Å for the high-spin compounds [Co(saloph)(2-MeImd)] (0.45 Å)[23] and [Co(3-MeOsalen)(H_2O)] (0.43 Å).[28] The three compounds reported in this paper show a high-spin configuration and all of them show an important out-of-plane displacement of the Co^{II} ion of ca. 0.6–0.74 Å. The high value

Table 4. Comparison of the ZFS parameters and distortions for high-spin five-coordinate Co^{II} complexes.

	Core	$\|D\|$ [cm^{-1}]	g	$-zJ$ [cm^{-1}]	τ[b]	Ref.
[Co(S-dept)Br_2]	$CoNS_2Br_2$	20.5	2.53	0.5	0.36	[c]
[Co(S-dept)I_2]	$CoNS_2I_2$	14.2	2.38	1.67	0.58	[c]
[Co(S-dept)$(NCS)_2$]	$CoNN'_2S_2$	17.7	2.35	1.23	0.43	[c]
[Co(*t*Bu)(Me)(salmdptn)]	CoO_2N_2N'	38.9	2.26[a]	1.0	0.64	[22]
[Co(saloph)(2-MeImd)]	CoO_2N_2N'	22.6	2.14		0.19	[23]

[a] $g = (gx + gy + gz)/3$. [b] $\tau = 1$: trigonal-bipyramid; $\tau = 0$: square pyramid.[38] [c] This work.

of this displacement could be attributed to the different nature of the ligands in the basal plane: N_2O_2 for salen and saloph and NS_2X for compounds **1**–**3**. The presence of a voluminous donor-atom ligand favors the distortion and stabilize the $S = 3/2$ state.

In the same way, Hitchaman showed[46] that increasing distortions from a square-pyramidal geometry could lead to a rapid decrease in the quartet-state energy, especially when $\beta > 102°$ ($\beta = L_{ax}$–Co–N angle). For the three compounds reported in this paper, the largest β angle is found for the iodo complex **2** with $\beta = 107°$ (major distortion to the trigonal-bipyramidal geometry); for **1** and **3** the β angle is slightly more than 90° (91.7° and 93.6°, respectively).

In comparison with the Schiff-base complexes, compounds **1**–**3** show a major distortion in the geometry: the presence of the *S*-dept ligand, with its sulfur atom coordinated to the Co^{II} ion favors the out-of-plane displacement of the metal center. Due to the tridentate character of the *S*-dept ligand, the fourth position of the basal plane is occupied by a monodentate ligand, consequently a major flexibility of the geometry could be attended. The most voluminous monodentate ligand, iodide, leads to a major distortion from the square-pyramidal to the trigonal-bipyramidal geometry. Therefore, in the reported compounds [Co(S-dept)X_2] (**1**–**3**) both ligands, *S*-dept and X, favor the stabilization of the $S = 3/2$ state in preference to the $S = 1/2$ state.

For systems with an $S = 3/2$ state, the magnetic anisotropy due to the non-spherical distribution of the spin density is enhanced by the low symmetry of the five-coordinate chromophore. The D values found for compounds **1**–**3** are of the same order as reported for other five-coordinate Co^{II} complexes with $S = 3/2$. Attempts to correlate the zero-field splitting parameter (D) with the structural distortions are hard, due to the limited number of compounds of this kind reported in the literature. Compounds **1**–**3** show quite smaller D and g values than [Co{(*t*Bu)(Me)salmdptn}][22] and [Co(saloph)(2-MeImd)][23] (Table 4).

It is difficult to interpret the differences in the zero-field splitting parameters for five-coordinate Co^{II} complexes. The magnitude of D and g values is influenced by the second-order spin-orbit coupling, λ and $1/\Delta_i$, where λ is the spin-orbit coupling constant and Δ_i the energy gap between ground state and excited states. The expression of the axial ZFS parameter $D = f(\lambda, 1/\Delta_i)$ for different ions and geometries could be found in a recent review about the zero-field splitting in metal complexes.[47] For Co^{II} ions, the equation for the d^7 ion in a tetrahedral environment is also described in this paper, but not for a five-coordinate complex.

For a free Co^{II} ion $\lambda = -180$ cm^{-1}. But this parameter is sensitive to the covalence of the bond. Compounds **1**–**3** with the *S*-dept ligand must show a greater degree of covalence than the compounds with Schiff-base ligands. Thus, a lower $|\lambda|$ value must be expected for compounds **1**–**3**. Complex **2** with iodide as monodentate ligand, should show a maximum covalence in the Co–X bonds, and consequently the small $|\lambda|$ value must correspond to this compound.

On the other hand, the D value is sensitive to the proximity of excited states with orbital contribution. Several factors influence the energy gaps, Δ_i, such as the bond covalence, the kind of donor atom and the distortions in geometry. In spite of the limitations of the extended Hückel calculations, the presence of several excited states at low energy could be attended. However, the inter-electronic repulsion must be different for the three complexes, due to the presence of different X ligands (Br, I, NCS), and it is not precise to compare the energy values of the excited states postulated in Table 3. The presence of excited states at low energy contributes to the D value, but it is not possible to rationalize their effect.

Compounds formed by voluminous donor ligands such as *S*-dept or iodide, could contribute to diminish the zero-field splitting (small $|D|$ values). Compounds **1**–**3** show lower values than the compounds with Schiff-base ligands.[22,23] Therefore, complex **2** containing S-dept and iodide exhibits the lowest $|D|$ value.

On the other hand, it is difficult to correlate the distortion of the coordination polyhedron with the zero-field splitting parameter. For the two complexes with Schiff-base ligands the compound with major distortion from the square-pyramidal geometry (larger τ) show a larger D value, while for the three complexes reported here with the *S*-dept ligand, the maximum τ value corresponds to compound **2**, with the lowest value of the zero-field splitting parameter.

EPR Spectra

The EPR spectra of powdered samples and of frozen CH_2Cl_2 solution of **1**–**3** were recorded at different temperatures. Only below 100 K was the EPR signal significant, due to the relaxation effects.

The EPR spectra of powdered samples show in all cases a very broad band, with a better resolution at 4 K. The most intense features were found at low field, in the region of 2000 G. In frozen solution the three compounds show very similar spectra (Figure 7) with the most intense feature

at ca. 1200 G ($g \approx 5.5$). The position of this band is similar for the three compounds (1150 G for **1**, 1250 G for **2**, and 1180 G for **3**). Another small feature was observed at 2760 G. The low-field signal can be attributed to $g_{\perp}$ and the small signal centred at ca. 2800 G to $g_{\|}$. These spectra are characteristic of a high-spin Co^{II} complex, with S = 3/2 and a large zero-field splitting ($D > g\beta H$), as occurs in compounds **1**–**3** whose $|D|$ values are between 14–21 cm^{-1}.

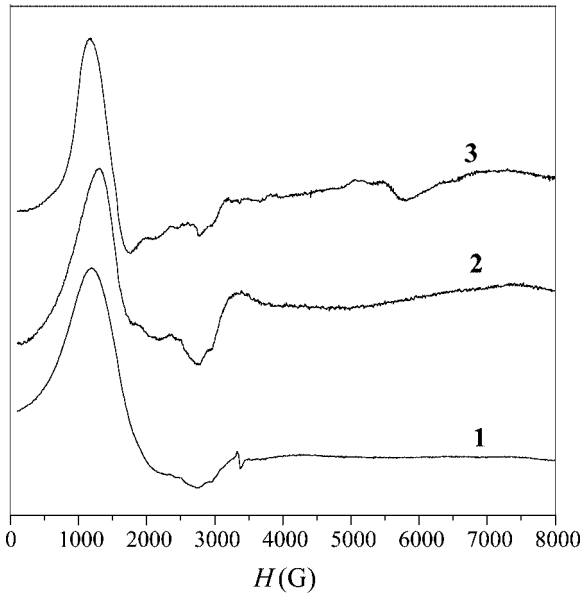

Figure 7. X-band EPR spectra of frozen CH_2Cl_2 solutions of complexes **1**–**3**.

Conclusions

In this work we have reported the synthesis and characterization of three new five-coordinate Co^{II} complexes. In all cases, the coordination polyhedron of the Co^{II} ion is a distorted square pyramid, with an electronic configuration of high-spin. Although there is no correlation between the angle of rotation of thioamide groups and the pyridine ring, the conformation of the ligand is dependent on the size of the anion. The compounds show major distortion in the geometry with a large out-of-plane displacement of the Co^{II} ion of ca. 0.6–0.74 Å. The distortion of the geometry, due to the *S*-dept ligand with voluminous donor atoms, could explain the stabilization of the S = 3/2 state than the S = 1/2 state.

Important zero-filed splitting is observed, as it could be expected for high-spin Co^{II} compounds. The D value seems to be very sensitive to the nature of the ligand. The compounds reported in the literature, with a CoO_2N_2 core show larger $|D|$ values than compounds **1**–**3**, with a $CoNS_2X_2$ core. The smallest value corresponds to compound **2** containing more diffuse donor atoms ($CoNS_2I_2$ core) with maximum covalence of the Co–L bonds.

The EPR spectra at low temperature show two bands, at low fields, characteristic of systems with an S = 3/2 ground state and an important zero-field splitting, as is the case for Co^{II} compounds.

Experimental Section

Materials: All reactions were carried out under anhydrous conditions. Solvents were dried using standard techniques. Absolute ethanol (AR quality, Hayman Ltd.) and pyridine-2,6-dicarboxylic acid (Fluka) were used as supplied. *N*,*N*,*N*′,*N*′-Tetraethylpyridine-2,6-dithiocarboxamide was prepared as described earlier.[7,8]

Synthesis of the Complexes [Co(S-dept)X_2] [X = Br (1), I (2) and NCS (3)]: $CoCl_2$ (3 mmol), dissolved in anhydrous ethanol (20 mL), was added to a solution of KBr or KI or KSCN (each 6 mmol) in ethanol (20 mL). The mixture was refluxed for about 4 h. The white precipitate of KCl was removed by filtration and *S*-dept (3 mmol), dissolved in ethanol (20 mL), was added to the solution. After refluxing for about 4–5 h, **1**, **2** and **3** were obtained as dark green solids on keeping at room temperature. The complexes were crystallized from anhydrous ethanol by slow concentration at room temperature. **1:** Yield 1.36 g (86%). M.p. 210 °C. $C_{15}H_{23}Br_2CoN_3S_2$ (528): calcd. C 34.09, H 4.35, Br 30.3, N 7.95; found C 33.92, H 4.12, Br 29.8, N 8.10. Conductivity (ca. 1 mM solution at 298 K): Λ_M = 32 (MeCN) and 24 (DMF) Ω^{-1} cm^2·mol^{-1} (expected range for 1:1 electrolytes in MeCN and DMF is 120–160 and 65–90 Ω^{-1} cm^2·mol,$^{-1}$ respectively). UV/Vis [10^{-3} cm^{-1}]: λ = 19.8, 17.0, 13.7, 11.0 ($CHCl_3$); 15.7, 14.9 (DMF); 23.5, 16.6, 10.0, 5.9 (solid). Selected IR frequencies (KBr disk [cm^{-1}]): ν̃ = 1600, 1579, 1530, 1463, 1442, 1316, 1310, 1275, 1252, 1186, 1170, 1149, 1097, 1073, 1000, 978, 914, 809, 762, 746, 723, 682, 662, 648, 508, 488, 454. **2:** Yield, 1.79 g (87%). M.p. 242 °C. $C_{15}H_{23}CoI_2N_3S_2$ (622): calcd. C 28.93, H 3.69, I 40.8, N 6.75; found C 28.78, H 3.57, I 40.3, N 6.54. Conductivity (ca. 1 mM solution at 298 K): Λ_M = 95 (MeCN) and 67 (DMF) Ω^{-1} cm^2·mol^{-1}. UV/Vis [10^{-3} cm^{-1}]: λ = 17.4, 15.6, 13.6, 9.3 ($CHCl_3$); 19.0, 15.0 (DMF). Selected IR frequencies (KBr disk [cm^{-1}]): ν̃ = 1600, 1584, 1534, 1463, 1444, 1410, 1314, 1277, 1255, 1186, 1165, 1144, 1097, 1073, 1002, 980, 910, 806, 759, 746, 722, 680, 666, 632, 510, 486, 450. **3:** Yield 1.47 g (87%). M.p. 205 °C. $C_{17}H_{23}N_5S_4Co$ (484): calcd. C 42.14, H 4.75, N 14.46, S 26.4; found C 42.02, H 4.54, N 14.28, S 26.1. Conductivity (ca. 1 mM solution at 298 K): Λ_M = 30 (MeCN) and 25 (DMF) Ω^{-1} cm^2·mol^{-1}. UV/Vis [10^{-3} cm^{-1}]: 17.2, 15.6, 14.2 ($CHCl_3$); 17.2, 16.0 (DMF); 23.5, 17.1, 11.1, 5.9 (solid). Selected IR frequencies (KBr disk [cm^{-1}]): ν̃ = 2062, 1600, 1580, 1530, 1460, 1438, 1410, 1315, 1277, 1259, 1187, 1164, 1144, 1094, 1072, 1010, 980, 909, 812, 722, 668, 640, 562, 478, 456, 424.

Physical Methods: Elemental analyses (C,H,N) were carried out with a Perkin–Elmer model 2400 CHN elemental analyzer at the SAIF, Panjab University. Bromide and iodide anions were determined by precipitation as silver salts and sulfur by precipitation as $BaSO_4$. IR spectra were recorded as KBr pellets with a Perkin–Elmer RX-1 FTIR spectrophotometer. Molar conductances were measured using a Digital conductivity bridge, Model CC601.The UV/Vis spectra were recorded with a JASCO V-530 UV/Vis spectrophotometer in a 1-cm matched quartz cell. The diffuse reflectance spectra of powdered samples were recorded with a Hitachi Model 330 integrating sphere reflectance spectrophotometer in the 185–2600 nm region, using magnesium oxide as reference. Magnetic susceptibility measurements, for polycrystalline samples of **1**–**3**, were performed with a Quantum Design SQUID MPMS-XL susceptometer, working in the range 2–300 K under magnetic fields of 2000 G, at the "Servei de Magnetoquímica" (Universitat de Barcelona). Pascal's constants were used to estimate the diamagnetic

Table 5. Crystal data and structure refinement parameters for complexes **1**–**3**.

	Complex **1**	Complex **2**	Complex **3**
Emperical formula	$C_{15}H_{23}Br_2CoN_3S_2$	$C_{15}H_{23}I_2CoN_3S_2$	$C_{17}H_{23}CoN_5S_4$
Formula mass	528.23	622.21	484.57
Temperature	293(2) K	293(2) K	293(2) K
Wavelength	0.71073 Å	0.71073 Å	0.70930 Å
Crystal system, space group	triclinic, $P\bar{1}$	monoclinic, $P2_1/c$	triclinic, $P\bar{1}$
Unit-cell dimensions	a = 8.434(1) Å, α = 91.40(1)°	a = 12.824(1) Å, α = 90°	a = 8.6220(9) Å, α = 88.277(6)°
	b = 10.330(1) Å, β = 108.58(1)°	b = 14.967(1) Å, β = 92.88(1)°	b = 11.4370(8) Å, β = 80.842(7)°
	c = 13.220(1) Å, γ = 113.56(1)°	c = 11.092(1) Å, γ = 90°	c = 12.1540(9) Å, γ = 81.312(7)°
Volume	985.34(17) Å^3	2126.3(3) Å^3	1169.63(17) Å^3
Z, calculated density	2, 1.780 Mg/m^3	4, 1.944 Mg/m^3	2, 1.376 Mg/m^3
Absorption coefficient	5.139 mm^{-1}	3.909 mm^{-1}	1.102 mm^{-1}
F(000)	526	1196	502
Crystal size	0.24 × 0.20 × 0.16 mm	0.28 × 0.24 × 0.19 mm	0.2 × 0.2 × 0.1 mm
θ range for data collection	2.18–23.99°	2.09–24.00°	1.69–24.96°
Scan type	2θ-θ	2θ-θ	2θ-θ
Scan speed	variable, 2.0–60.0°/min in ω	variable, 2.0–60.0°/min in ω	variable, 2.0–60.0°/min in ω
Limiting indices	$0 \le h \le 9$	$-14 \le h \le 14$	$0 \le h \le 10$
	$-11 \le k \le 10$	$0 \le k \le 17$	$-13 \le k \le 13$
	$-15 \le l \le 14$	$0 \le l \le 12$	$-14 \le l \le 14$
Reflections collected/unique	3270/3012 [R(int) = 0.0309]	3546/3342 [R(int) = 0.0190]	3602/3602 [R(int) = 0.0147]
Refinement method	Full-matrix least squares on F^2	Full-matrix least squares on F^2	Full-matrix least squares on F^2
Data/restraints/parameters	3012/0/208	3342/0/208	3602/0/244
Goodness-of-fit on F^2	1.012	1.012	1.053
Final R indices [$I > 2\sigma(I)$]	R_1 = 0.0747, wR_2 = 0.2200	R_1 = 0.0383, wR_2 = 0.1093	R_1 = 0.0535, wR_2 = 0.1422
R indices (all data)	R_1 = 0.0804, wR_2 = 0.2275	R_1 = 0.0420, wR_2 = 0.1127	R_1 = 0.0668, wR_2 = 0.1534
Largest difference peak/hole	2.051/–1.579 e·Å^3	0.930/–1.670 e·Å^{-3}	0.765/–0.363 e·Å^{-3}

corrections. The fits were performed by minimizing the function $R = \Sigma[(\chi_M T)_{exp} - (\chi_M T)_{cal}]^2/\Sigma(\chi_M T)_{exp}^2$. EPR spectra for **1**–**3** were recorded at X-band (9.4 GHz) frequency with a Bruker ESP-300E spectrometer from room temperature to 4 K, at the "Servei de Magnetoquímica" (Universitat de Barcelona).

X-ray Crystallography: Crystallization of **1**, **2** and **3** by slow concentration of their saturated ethanolic solutions at room temperature yielded good single crystals. Intensity data were collected with a Siemens P4 single-crystal diffractometer equipped with a molybdenum sealed tube (λ = 0.7173 Å) and highly oriented graphite monochromator. Table 5 shows the unit cell parameters and data measurement details. The parameters associated with the structure of **1** are as follows: Crystal size 0.24 × 0.20 × 0.16 mm. The lattice parameters and standard deviations were obtained by least-squares fit to 40 reflections $10.085° < 2\theta < 30.312°$ The data were collected by the 2θ-θ scan mode with a variable scan speed ranging from 2.0 to a maximum of 60° min^{-1}. Three reflections were used to monitor the stability and orientation of the crystal and were measured after every 97 reflections. Their intensities showed only statistical fluctuations during 40.28 h of X-ray exposure time. The data were collected for Lorentz and polarisation factors and an empirical absorption correction based on the ψ-scan method was applied. The structure was solved by direct methods using SHELX-97[34] and also refined on F^2 using the same one. All non-hydrogen atoms were refined anisotropically. The hydrogen atoms were included in the ideal positions with fixed isotropic U values and were riding on their respective non-hydrogen atoms. A weighting scheme of the form $w = 1/[(\sigma^2F_o^2) + (ap)^2 + bp]$ with a = 0.1606 and b = 8.27 was used. The refinement converged to a final R value of 0.0747 (wR_2 = 0.22 for 3012 reflections) [$I > 2\sigma(I)$]. The final difference map was featureless. The data collection procedure, structure solution and refinement for compounds **2** and **3** were essentially the same as for **1**. The parameters associated with the structures are as follows: **2:** 40 reflections $(0.420° < 2\theta < 30.118°)$ for an accurate cell parameter determination, crystal size 0.28 × 0.24 × 0.19 mm, a total of 46.90 h of X-ray exposure time, R = 0.0383 (wR_2 = 0.1093 for 3342 reflections) [$I > 2\sigma(I)$] with a = 0.0572 and b = 10.73 in weighting scheme. **3:** 40 reflections $(0.420° < 2\theta < 30.118°)$ for an accurate cell parameter determination, crystal size 0.20 × 0.20 × 0.10 mm, a total of 48 h of X-ray exposure time, R = 0.0535 (wR_2 = 0.1422 for 3602 reflections) [$I > 2\sigma(I)$] with a = 0.0811 and b = 1.8505 in above mentioned weighting scheme. A summary of the crystal parameters, experimental details and refinement results are listed in Table 5. CCDC-254292 (**1**), -254293 (**2**), and -254294 (**3**) contain the supplementary crystallographic data for this paper. These data can be obtained free of charge from The Cambridge Crystallographic Data Centre via www.ccdc.cam.ac.uk/data_request/cif.

Acknowledgments

A. K. is grateful to CSIR New Delhi, India for a Senior Research Fellowship. The authors thank MEC of Spain (project BQ2003-00538) for financial support.

[1] S. L. Jain, P. Bhattacharyya, H. L. Milton, A. M. Z. Slawin, J. A. Crayston, J. D. Woollins, *Dalton Trans.* **2004**, 862–871.
[2] a) T. Le Borgne, P. Altmann, N. Andre, J.-C. G. Bunzli, G. Bernardinelli, P. Morgantini, J. Weber, C. Piguet, *Dalton Trans.* **2004**, 723–733; b) T. Le Borgne, J.-M. Benech, S. Floquet, G. Bernardinelli, C. Aliprandini, P. Bettens, C. Piguet, *Dalton Trans.* **2003**, 3856–3868; c) F. Renaud, C. Piguet, G. Bernardinelli, J.-C. G. Bunzli, G. Hopfgartner, *Chem. Eur. J.* **1997**, *3*, 1646–1659.
[3] J. Garcia-Lozano, M. A. Martinez-Lorente, E. Escriva, R. Ballesteros, *Synth. React. Inorg. Met.-Org. Chem.* **1994**, *24*, 365–376.
[4] J. Garcia-Lozano, L. Soto, J. V. Folgado, E. Escriva, *Polyhedron* **1996**, *15*, 4003–4009.
[5] J. G. H. du Preez, B. Van Breeht, *Inorg. Chim. Acta* **1989**, *162*, 49–56.

[6] J. G. H. du Preez, B. Van Breeht, J. F. de Wet, J. Koorts, *Inorg. Nucl. Chem. Lett.* **1974**, *10*, 935–939.
[7] R. Kapoor, A. Kataria, P. Kapoor, P. Venugopalan, *Trans. Met. Chem.* **2004**, *29*, 425–429.
[8] R. Kapoor, A. Kataria, P. Venugopalan, P. Kapoor, M. Corbella, M. Rodriguez, M. Romero, M. Sola, A. Llobet, *Inorg. Chem.* **2004**, *43*, 6699–6706.
[9] K. R. Justin Thomas, V. Chandrasekhar, S. R. Scott, A. W. Cordes, *Polyhedron* **1995**, *14*, 1607–1613.
[10] C. Arici, D. Veku, R. Kurtaran, K. C. Emergl, O. Atakol, *Z. Kristallogr.* **2003**, *218*, 497–500.
[11] Z. Dori, R. Eisenberg, H. B. Gray, *Inorg. Chem.* **1967**, *6*, 483–486.
[12] E. Goldschmied, N. C. Stephenson, *Acta Crystallogr. Sect. B* **1970**, *26*, 1867–1875.
[13] M. Gerloch, *J. Chem. Soc. A* **1966**, 1317–1325.
[14] L. Sacconi, R. Morassi, S. Midollini, *J. Chem. Soc. A* **1968**, 1510–1515.
[15] Z. Dori, H. B. Gray, *Inorg. Chem.* **1968**, *7*, 889–892.
[16] M. Ciampolini, N. Nardi, *Inorg. Chem.* **1966**, *5*, 41–44; M. Ciampolini, N. Nardi, *Inorg. Chem.* **1966**, *5*, 1150–1154.
[17] L. Sacconi, I. Bertini, R. Morassi, *Inorg. Chem.* **1967**, *6*, 1548–1553.
[18] M. Ciampolini, G. P. Speroni, *Inorg. Chem.* **1966**, *5*, 45–49.
[19] M. Di Vaira, P. L. Orioli, *Chem. Commun.* **1965**, 590.
[20] F. Tuna, L. Patron, E. Rivière, M. Boillot, *Polyhedron* **2000**, *19*, 1643–1648.
[21] D. V. Naik, W. R. Scheidt, *Inorg. Chem.* **1973**, *12*, 272–276; M. G. B. Drew, A. H. bin Othman, S. G. McFall, P. D. A. McIlroy, S. M. Nelson, *J. Chem. Soc. Dalton Trans.* **1977**, 438–446.
[22] R. Boca, H. Elias, W. Haase, M. Hüber, R. Klement, L. Müller, H. Paulus, I. Svoboda, M. Valko, *Inorg. Chim. Acta* **1998**, *278*, 127–135.
[23] B. J. Kennedy, G. D. Fallon, B. M. K. C. Gatehouse, K. S. Murray, *Inorg. Chem.* **1984**,*23*, 580–588.
[24] A. Garoufis, S. Kasselouri, C. P. Raptopoulou, *Inorg. Chem. Commun.* **2000**, *3*, 251–254.
[25] C. Bianchini, G. Mantovani, A. Meli, F. Migliacci, F. Zanobini, F. Laschi, A. Sommazzi, *Eur. J. Inorg. Chem.* **2003**, 1620–1631.
[26] A. K. Patra, M. Ray, R. Mukherjee, *J. Chem. Soc. Dalton Trans.* **1999**, 2461–2466.
[27] T. M. Kooistra, K. F. W. Hekking, Q. Knijnenburg, B. de Bruin, P. H. M. Budzelaar, R. de Gelder, J. M. M. Smits, A. W. Gal, *Eur. J. Inorg. Chem.* **2003**, 648–655.
[28] M. Calligaris, G. Nardin, L. Randaccio, *J. Chem. Soc. Dalton Trans.* **1974**, 1903–1906.
[29] L.-J. Zhang, X.-L. Zhao, P. Cheng, J.-Q. Xu, X. Tang, X.-B. Cui, W. Xu, T.-G. Wang, *Bull. Chem. Soc. Jpn.* **2003**, *76*, 1179–1184.
[30] L.-Y. Wang, B. Zhao, C.-X. Zhang, D. Z. Liao, Z.-H. Jiang, S.-P. Yan, *Inorg. Chem.* **2003**, *42*, 5804–5806.
[31] U. Beckmann, S. Brooker, C. V. Depree, J. D. Ewing, B. Moubaraki, K. S. Murray, *J. Chem. Soc. Dalton Trans.* **2003**, 1308–1313.
[32] T. Whitfield, L.-M. Zheng, X. Wang, A. J. Jacobson, *Solid State Sci.* **2001**, 829–835.
[33] R. Kapoor, A. Kataria, A. Pathak, P. Venugopalan, G. Hundal, P. Kapoor, *Polyhedron* **2005**, *24*, 1221–1231.
[34] G. M. Sheldrick, *SHELX-97, Program for solution and refinement of crystal structures*, University of Göttingen, Göttingen, Germany, **1997**.
[35] W. J. Geary, *Coord. Chem. Rev.* **1971**, *7*, 81–122.
[36] N. N. Greenwood, K. Wade, *J. Chem. Soc.* **1960**, 1130–1141.
[37] P. C. H. Mitchell, R. J. P. Williams, *J. Chem. Soc.* **1960**, 1912–1918; J. Lewis, R. S. Nyholm, P. W. Smith, *J. Chem. Soc.* **1961**, 4590–4599; J. L. Burmeister, *Coord. Chem. Rev.* **1966**, *1*, 205–221; J. L. Burmeister, *Coord. Chem. Rev.* **1968**, *3*, 225–245.
[38] D.-T. Wu, C.-S. Chung, *Inorg. Chem.* **1986**, *25*, 3584–3587.
[39] A. W. Addison, T. N. Rao, J. Reedijk, J. Vm Riju, G. C. Verschoor, *J. Chem. Soc. Dalton Trans.* **1984**, 1349–1356.
[40] S. E. Livingstone, *Q. Rev. Chem. Soc.* **1965**, *19*, 386–425.
[41] L. P. Battaglia, A. Bonamartini Corradi, A. Mangia, *Inorg. Chim. Acta* **1980**, *39*, 211–216.
[42] M. G. B. Drew, A. H. bin Othman, S. M. Nelson, *J. Chem. Soc. Dalton Trans.* **1976**, 1394–1399.
[43] P. Paoletti, M. Ciampolini, *Inorg. Chem.* **1967**, *6*, 64–68.
[44] Package of programs for Molecular Orbital Analysis. C. Mealli, D. M. Proserpio, *J. Chem. Educ.* **1990**, *67*, 399.
[45] O. Kahn, *Molecular Magnetism*, VCH, New York, **1993**.
[46] M. A. Hitchman, *Inorg. Chim. Acta* **1978**, *26*, 237–245.
[47] R. Boca, *Coord. Chem. Rev.* **2004**, *248*, 757–815.

Received: April 17, 2005
Published Online: August 10, 2005

